POSTER: Duct tracking in 3D medical data

Martin Petříček
Faculty of Mathematics and Physics
Charles University, Prague
Malostranské nám. 25, 11800 Praha 1,
Czech Republic
martin@petricek.net

Josef Pelikán
Faculty of Mathematics and Physics
Charles University, Prague
Malostranské nám. 25, 11800 Praha 1,
Czech Republic
Josef.Pelikan@mff.cuni.cz

Martin Horák
Department of Radiology,
Bulovka Hospital, Prague
Budínova 2, 180 81 Praha 8 - Libeň
Czech Republic
martin.horak@volny.cz

ABSTRACT

Implementing duct tracking of bronchi and blood vessels in 3D medical data can significantly help in examining these body structures and reduce time needed for correct diagnosis. Nature of the problem involved may require some operator interaction when selecting duct branches of interest or correcting possible mistakes in duct path segmentation. Noise, badly discernible duct walls, branching or extreme duct curvatures, that can be found in computer tomography data, make the segmentation challenging. There are more ways to display segmented ducts, as overlay over original data or unrolled to planar tube, allowing easier measurements of length, width or observation of tube anomalies.

Keywords: Image segmentation, visualization, 3D medical data, computer tomography.

1 INTRODUCTION

Examination of human body with computer tomography or magnetic resonance allows to see inside a patient. Unlike X-ray imaging these measurements provide full 3D data, which requires specialized program to view or visualize them.

In this paper we specialize on duct tracking. This include ducts in respiratory system (trachea, bronchi), blood vessels (veins, arteries) and possibly gastrointestinal tract.

First type are bronchi - tubular structures in respiratory system, usually filled with air, although they can be relatively commonly blocked by various inhaled objects. Bronchi are probably easier for segmentation, as they usually contain only air and are the simplest to segment.

Second type of ducts in human body are blood vessels - veins and arteries. They are used to transport blood in human body. Sometimes a contrast agent, such as Ultravist, is applied to enhance the density of blood in veins. This make them more contrast and thus more visible, as we can see in example in Figure 2. In the image without contrast agent the artery blends with surrounding tissues of similar density. With contrast agent applied, the artery is clearly visible. Quite common feature that can be found in blood vessels is thrombus. The

Figure 1: Following ducts in CT data can be tedious.

thrombus has almost the same density as blood, so it is generally visible only with help of contrast agent.

Third type is gastrointestinal tract (small and large intestine). These are the hardest to segment. They can contain liquid or solid content, or even pockets of gas, which can make segmentation problematic, as they have highly varying densities. Intestines have thin, badly visible walls, the curvature and circumference is varying largely as the intestine continues through the body and the intestines often touch themselves as they are folded in the abdominal area. Example of slice showing part of gastrointestinal tract can be seen in Figure 3
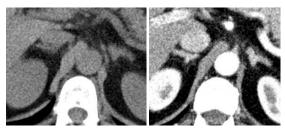
Figure 2: Blood vessel (aorta) - left image is slice from data without contrast agent, right image is from data with contrast agent (Ultravist) applied
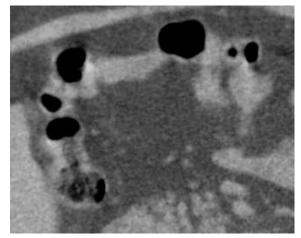

Figure 3: Image from gastrointestinal tract with visible pockets of gas, example of very hard segmentation problem

2 PROBLEM DECOMPOSITION

We have analyzed the problem and decomposed it into multiple consecutive steps.
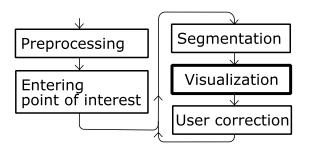

Figure 4: Problem decomposition into separate steps

First optional step is preprocessing. It may improve the segmentation and the resulting image if some filters to reduce noise are used, as CT and MRI tend to be generally noisy. Three dimensional variant of Averaging using a rotating mask [SHB93] with $3 \times 3 \times 3$ masks in $5 \times 5 \times 5$ area can be used, as it preserve edges. Its disadvantage is computational intensity, because for each voxel, brightness dispersion σ^2 needs to be computed for each rotated mask. Median filtering is faster, for $3 \times 3 \times 3$ mask by factor of 7.30, for $5 \times 5 \times 5$ by factor of 1.65. Disadvantage of median filtering can be round-

ing of sharp corners, but that might not be noticeable in most anatomy images. Both noise-removing filters can be run on series of slices as 2D filters, or extended to fully 3D filter.

As the image is usually relatively much larger than the area of interest, it is possible to reduce time needed for preprocessing. Preprocessing can be run only on a small area around the starting point and then on neighbor areas, as the segmentation continues and tracks the duct through the body. As result, the computationally expensive filter will be run only on areas that are close to the area of interest.

Second step is entering point of interest. Basically, there are many ducts in human body and user must pick some starting point inside the duct in which he is interested and direction in which to track it.

For some types of images and few specific cases, the starting point can be recognized automatically and may be offered as a preselection (like position of trachea on image from chest area).

Third step is the segmentation. The hard part is finding the duct walls. Once duct walls are identified, finding the axis (centerline) and inside volume is quite straightforward.

Segmentation and visualization will be discussed with greater detail in next two chapters

Fourth step is visualization. There are more possible ways for showing resulting ducts. Either they can be highlighted in 3D view of original data or they can be unwinded and displayed separately. Unwinded duct still remain a 3D image, though.

Fifth and the last step is correction. As ducts in body often have branches, user have to pick one of the ways. Also, there will be cases in which the segmentation was incorrect and algorithm has left the duct. These should be corrected. The algorithm should continue following the proper duct after adjustment, basically running again on part of the duct from third step with modified parameters. This requires functions in visualization part that enable user to specify the corrections.

Another possibility is to segment entire duct tree, forking the segmentation at every duct split. Entire bronchi system can be segmented and then displayed or measured this way.

3 SEGMENTATION

Segmentation is still work in progress. Most promising are Active Shape models, also called "snakes": [CT92], [dBvGVN03], or its variant, Active Appearance Models [CET98]. There are many variations to these methods: [XP97], [CC93], [OBFG94], [Coh91].

They are contour models, attracted to image features, such as edges. The contour is usually represented as a spline curve and often there are imposed limits on the deformation to ensure it maintain "reasonable" shape.
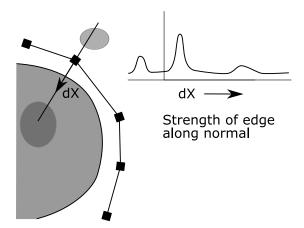
Figure 5: Points on the curve are moved towards strongest edge, proportional to its strength. The process is repeated for each point until the curve converges to approximate the object contour

Figure 6: Branching of aorta, with contrast agent applied. Left image show situation from above, right image shows it from side

$$p_0 = initial\ position$$
$$d_0 = initial\ direction$$
$$d_0 = correct\ orientation(p_0, d_0)$$
$$w_0 = find\ duct\ walls(p_0, d_0)$$
$$p_0 = duct\ center(w_0)$$
for $i = 1..length\ of\ duct$ **do**
$$\quad p_i = p_{i-1} + d_{i-1}$$
$$\quad d_i = d_{i-1}$$
$$\quad w_i = find\ duct\ walls(p_i, d_i, w_{i-1})$$
$$\quad p_i = duct\ center(w_i)$$
$$\quad d_i = p_i - p_{i-1}$$
Array p_i holds positions
Array d_i hold directions
Array w_i holds walls slices

Algorithm 1: Pseudo-code of segmentation algorithm. "find duct walls" is the main algorithm to segment the walls, given the 2D slice specified by (p,d) and position of duct walls in previous slice (except the first slice, where the initial duct must be found some other way)

In the algorithm, first the initial curve is placed in the data - for tubes it will be initially a circle, or shape of the tube from previous slice. Then, the algorithm step is repeated, until the model converges. In each step, every point is moved towards strongest nearby edge along the normal of the contour in that point. This results in the contour following the edge.

The model needs to be extended to 3D data and slices that are generally not parallel to any major axis or to other slices.

Another possible approach is not to use 2D deformable models on moving slices, but use instead a 3D deformable model (possibly trying to fit a cylinder on the duct walls). Advantage of such approach is having surface representation directly as the result and we don't have to deal with artifacts that can result from extracting slices of arbitrary orientation from the data. As edge detector is part of the method, we also have to deal with data anisotropy. Very often the resolution of the data is not uniform, the voxel size in z axis, corresponding to the gap between image slices, is larger than in x and y axes. This is usually is problematic for many edge detectors. We may solve it by resampling the data, modifying the edge detector, or we can use edge detector that can work with anisotropic data, like method proposed by Brejl and Sonka[BS00].

More methods [Lak00] will be examined before deciding which one will be finally used.

For finding the first part of the duct, some other way must be used, as we have no previous duct slice. The position and direction may be somewhat inaccurate, as the user probably won't pinpoint exact center of the duct and its precise direction. We can use a variant of the method, where we allow tilting of the initial plane and try to minimize length of the curve (assuming minimal length is at the tube cross-section, this will compen-

sate for inaccurate initial direction). After successful segmentation, we can update the position to correspond to the centerline of the duct found. Sometimes it is hard to tell exactly what center is, but we use center of mass calculated from the duct walls for this purpose.

Result of duct segmentation from Algorithm 1 will be the centerline represented by series of points located approximately 1 voxel apart. A duct direction vector is defined in every such point. It is used as normal vector of plane for extracting a slice from the data. On each of these planes a border will be segmented, using information from last plane, since the planes are close to each other. As a result of one plane segmentation, centerline position and direction will be updated for next step.

By approximating the curves from all slices as a polygon and joining them it is possible to build polygonal 3D model of the duct. Alternatively, we can use B-splines, NURBS or similar smooth surface representation to get nicer results.
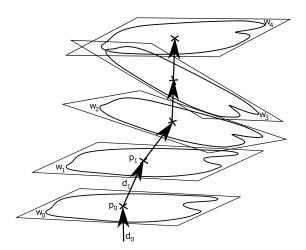
Figure 7: Example of one segmentation algorithm run, as specified by Algorithm 1. The segmentation starts on bottommost slice and moves upwards.

4 VISUALIZATION

There are two visualization modes, 3D mode and "duct unwinding" mode. In 3D mode, the segmented ducts will be highlighted in some way. Either by coloring the ducts, or by modifying transparency - so the ducts will be almost opaque, while the rest will be almost completely transparent. Both approaches could be combined. For the 3D mode, we will use part of MedV3D framework designed to display volume data.

In the second mode, slices are created along the duct center. Slices can be relatively small (width of the duct and some small part of surrounding tissue), but number of slices can be relatively large, if the duct is long. They are still displayed as 3D data, but in more comprehensible form.
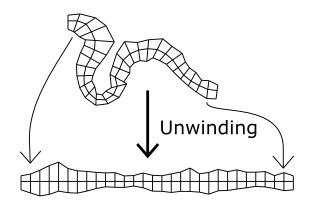

Figure 8: Schematic of "Duct unwinding" mode: Duct in original position is shown above, while corresponding unwinded duct is shown below. Length of centerline remain the same.

The deformation caused by unwinding will preserve lengths in each of the slices created and also length of the duct center will be preserved. Other lengths may be more or less deformed by the transformation, greatest deformation is in points farthest from centerline and in duct segments with greatest curvature.

Also, in this mode, specifying the corrections should be much easier than in ordinary 3D mode, as in case of bad segmentation, the correct duct leaving the resulting image can be easily spotted and corrected. See Figure 8 for simplified 2D schematic of how this mode will work. Once the duct is segmented, the data can be measured (for example volume of duct between certain points, its circumference, length, etc ...), as the voxel size is calibrated and its dimensions are part of the input data.

5 CONCLUSION AND FUTURE WORK

We have presented method for segmenting, measuring and displaying ducts in medical 3D images using deformable models, dealing with problems like anisotropy of the data, noise and irregularities in bodily ducts. The described approach aim to reduce time needed for proper patient diagnosis if bodily ducts are involved.

ACKNOWLEDGMENTS

REFERENCES

[BS00] Brejl, M. and Sonka, M. (2000). Directional 3d edge detection in anisotropic data: detector design and performance assessment. *Comput. Vis. Image Underst.*, 77(9):84–110.

[CC93] Cohen, L. and Cohen, I. (1993). Finite-element methods for active contour models and balloons for 2-d and 3-d images. *PAMI*, 15(11):1131–1147.

[Coh91] Cohen, L. D. (1991). On active contour models and balloons. *Computer Vision, Graphics, and Image Processing. Image Understanding*, 53(2):211–218.

[CT92] Cootes, T. and Taylor, C. (1992). Active shape models- - smart snakes.

[CET98] Cootes, T. F., Edwards, G. J., and Taylor, C. J. (1998). Active appearance models. *Lecture Notes in Computer Science*, 1407:484–??

[dBvGVN03] de Bruijne, M., van Ginneken, B., Viergever, M., and Niessen, W. (2003). Adapting active shape models for 3d segmentation of tubular structures in medical images.

[Lak00] Lakare, S. (2000). 3d segmentation techniques for medical volumes.

[OBFG94] O'Donnell, T., Boult, T., Fang, X., and Gupta, A. (1994). The extruded generalized cylinder: A deformable model for object recovery.

[SHB93] Sonka, M., Hlavac, V., and Boyle, R. (1993). *Image Processing, Analysis, and Machine Vision*. Chapman and Hall, London, New York.

[XP97] Xu, C. and Prince, J. (1997). Gradient vector flow: A new external force for snakes. In *Proceedings of Computer Vision and Pattern Recognition (CVPR '97)*, pages 66–71, San Juan, Puerto Rico. IEEE.